Int. J. Anal. Appl. (2026), 24:18

International Journal of Analysis and Applications

Time Series Decomposition and LSTM Neural Networks for Forecasting Transportation CO_2 Emissions in Saudi Arabia: Supporting Vision 2030 Climate Objectives

Dalia Kamal Alnagar[1,*], Abu Elgasim Abbas Abow Mohammed[2,6], Hussein Eledum[1], Sara Mohamed Ahmed Alsheikh[1], Elfarazdag M. M. Hussein[3], Rahmtalla Y. Yagoub[4], Walla Awad Maruod[5]

[1]*Department of Statistics, Faculty of Science, University of Tabuk, Kingdom of Saudi Arabia*
[2]*Department of Business Administration , College of Administrative Sciences and Humanities , Mustaqbal University, Kingdom of Saudi Arabia*
[3]*University College in Duba, University of Tabuk, Kingdom of Saudi Arabia*
[4]*Faculty of Umluj, University of Tabuk, Kingdom of Saudi Arabia*
[5]*Department of Mathematics, Faculty of Science, Al-Baha University, Kingdom of Saudi Arabia*
[6]*Department of Statistics, Faculty of Economic and Political Sciences, Omdurman Islamic University, Sudan*

[*]*Corresponding author:* d_alnajjar@ut.edu.sa

Abstract. This study develops an advanced forecasting framework by combining time series decomposition with Long Short-Term Memory (LSTM) neural networks to predict CO_2 emissions from Saudi Arabia's transportation sector through 2034, in support of Vision 2030 climate objectives. Using historical data from 1970 to 2024, the results show that LSTM models significantly outperform traditional ARIMA approaches, achieving superior accuracy with an error rate of 6.82% for total emissions compared to 13.51% for ARIMA. The analysis focuses on CO_2 emissions in three sectors: road transport, aviation transport, and total transport emissions. Findings indicate that road transport is the dominant source, contributing over 95% of total emissions, with projections rising from 149.8 million tons in 2025 to 172.5 million tons by 2034. Aviation emissions are expected to increase from 3.79 to 6.61 million tons over the same period, while total transport emissions reflect the combined upward trend of both sectors. Despite a gradual decline in annual growth rates, the persistent increase in emissions underscores the urgent need for sustainable transport policies, particularly those that promote electric vehicles and expanded public transit systems. The study's integration of STL decomposition

Received: Aug. 6, 2025.

2020 *Mathematics Subject Classification.* 62M10, 68T07.

Key words and phrases. LSTM neural networks; CO_2 emissions forecasting; time series decomposition; Saudi Arabia transportation; vision 2030; sustainable transportation; ARIMA comparison.

https://doi.org/10.28924/2291-8639-24-2026-18
ISSN: 2291-8639

with LSTM modeling provides a powerful, evidence-based tool for policymakers to guide CO_2 mitigation strategies and track progress toward Vision 2030 climate targets.

1. Introduction

The Kingdom of Saudi Arabia (KSA) needs to rapidly reduce CO_2 emissions from its growing transportation sector while also working towards its sustainability goals in accordance with the Vision 2030 framework [1]. To meet the multiple and dynamic needs of a green-planned economy, predicting emissions from the transport sector can help policymakers make optimal research-based decisions; therefore, it is essential to have a high level of precision. Accurate prediction of emissions from the transport sector is crucial for policymakers to make informed, research-oriented, and optimal decisions.

The portion of CO_2 emissions from the transport sector is consistently increasing in national emissions due to substantial population growth, with an average annual growth rate of 2.52%, and the consequent investment in transportation infrastructure [2].

The Saudi Arabian transportation sector is a vital pillar of the national economy and societal mobility, comprising extensive road, aviation, maritime, and emerging rail systems [3]. With over 221,000 km of roads and 12 million vehicles, road transport dominates, accounting for more than 95% of emissions due to high car ownership rates (400 vehicles per 1,000 people) [4]. Aviation, though a smaller emitter, remains economically significant with 27 airports handling more than 100 million passengers annually. As a global logistics hub, the Kingdom is pursuing ambitious Vision 2030 initiatives, including railway expansions, NEOM's sustainable transport projects, and electric vehicle infrastructure, to transform the sector's environmental footprint in the coming decades.

The time series of transport emissions for Saudi Arabia has shown nonlinear growth, multiple structural breaks after various economic events, and large fluctuations [5]. Traditional econometric and statistical approaches often exhibit suboptimal performance when faced with the complex set of temporal dependencies inherent in such time series of transport emissions. Consequently, the implementation of machine learning methodologies is required. One such method is the utilization of long-short-term memory (LSTM) neural networks. LSTM networks are well suited to capture intricate time series dynamics due to their unique architecture that can learn long-term dependencies and nonlinear relationships in the data [6,7].

The primary objective of this study is to investigate the historical trends and dynamics of CO_2 emissions in Saudi Arabia's transportation sector. It seeks to develop and implement an advanced predictive framework using LSTM neural networks to effectively model the nonlinear and long-term temporal dependencies inherent in emission data. By producing robust forecasts for the period 2025-2030, the study offers valuable insights to support environmental planning and policy development aligned with Saudi Arabia's Vision 2030 sustainability and climate objectives. In addition, its objective is to identify sector-specific emission drivers and assess the potential impact of future mitigation strategies, thereby supporting the development of a low carbon, sustainable transportation system.

This study is organized as follows: In Section 2, important research gaps are highlighted by reviewing the literature on time series decomposition, LSTM applications in environmental forecasting, and CO_2 emissions in Saudi Arabia. The methodology, including data preprocessing, LSTM model design, evaluation metrics, and decomposition analysis, is described in Section 3. The findings are presented in Section 4, which also compares the ARIMA and LSTM models and offers predictions for emissions from Aviation and road transport between 2025 and 2034. Section 5 concludes with a summary of the results, a discussion of the policy implications for Vision 2030, and suggestions and directions for further study.

2. Literature Review

This section examines the theoretical foundations and empirical evidence supporting the application of advanced forecasting methodologies to analyze transportation emissions. The review is organized into three main parts: time series decomposition techniques, which assist in preprocessing complex environmental data; LSTM neural networks, which have shown superior performance compared to other neural network architectures to predict environmental and energy outcomes; and existing research on CO_2 emissions in Saudi Arabia. By synthesizing findings from these related fields, the review highlights the rationale for adopting LSTM-based forecasting frameworks. Identifies critical research gaps that underpin the methodology and relevance of the current study.

2.1. **Time Series Decomposition in Environmental Modeling.** Time series decomposition has evolved as a fundamental preprocessing technique in environmental forecasting. Cleveland et al. [8] developed the seasonal and trend decomposition using the Loess (STL) approach, which has since become widely used due to its robustness in extracting underlying trends from noisy environmental data. Hyndman and Athanasopoulos [9] further highlighted the importance of decomposition in validating models and guiding their selection within comprehensive forecasting frameworks. Recently, Zhang et al. [10] conducted systematic reviews of decomposition methods in environmental forecasting, highlighting trend strength analysis as a critical factor in model architecture decisions. While Wang et al. [11] demonstrated a 15–25% improvement in forecast accuracy when combining STL decomposition with neural network approaches, effectively addressing the challenges of capturing both long-term trends and irregular patterns in emissions data.

2.2. **LSTM Applications in Environmental and Energy Forecasting.** LSTM neural networks have become popular as powerful tools for modelling nonlinear and complex environmental time series data due to their ability to overcome vanishing gradient problems and learn long-term dependencies. Alaraj et al. [12] utilized an ensemble tree-based machine learning model to forecast solar photovoltaic (PV) power in Qassim, Saudi Arabia, using meteorological data. The model demonstrated high accuracy based on RMSE, MAE, MSE, and MAPE, and outperformed other machine learning models. This work supports Saudi Vision 2030 by improving the reliability of the grid and promoting the integration of renewable energy.

Comparative studies between LSTM and its architectural variants have provided valuable insight into model selection for time series forecasting. da Silva and de Moura Meneses . [13] investigated the performance of standard LSTM and bidirectional LSTM (BiLSTM) networks in predicting power consumption, a domain closely related to emissions forecasting due to shared temporal complexity and variability. Their results indicated that BiLSTM models consistently outperformed traditional LSTM networks in terms of predictive accuracy, particularly in capturing both forward and backward temporal dependencies. The bidirectional structure enabled richer contextual learning and enhanced sensitivity to fluctuations and short-term patterns. These findings suggest that while standard LSTM remains effective, BiLSTM offers additional advantages in scenarios requiring nuanced temporal pattern recognition, insights that are directly applicable to the environmental forecasting of CO_2 emissions in transportation systems. Wu et al. [14] developed a DBO-LSTM model, integrating the Dingo Optimization Algorithm with LSTM networks, to improve the accuracy of the air quality index prediction (AQI). Their study showed that DBO-LSTM outperformed traditional models such as standard LSTM, RNN, and SVR in multiple performance metrics, including RMSE and R^2. By automatically optimizing the LSTM hyperparameters, the model achieved faster convergence and stronger generalization under highly dynamic environmental conditions. Although their focus was on air quality, the methodological framework aligns closely with the objective of this study of improving CO_2 emissions forecasting in the transportation sector. This reinforces the potential of optimization-enhanced LSTM models for future research on emission prediction, particularly in scenarios requiring adaptive learning under structural volatility.

2.3. **CO_2 Emissions Research in Saudi Arabia.** During the past two decades, several studies have examined the dynamics and drivers of CO_2 emissions in Saudi Arabia in various sectors, including energy, transportation, and industry. These studies have played a key role in identifying the underlying factors contributing to emissions and informing national sustainability policies. Alkhathlan and Javid [15] analyzed the links between economic growth and CO_2 emissions, revealing that industrial expansion exacerbates emissions, thus challenging the hypothesis of the environmental Kuznets curve in resource-dependent economies. Adenle and Alshuwaikhat [16] demonstrated the utility of spatial disaggregation for institutional-level emission analysis, but did not extend their findings to the transportation sector. These studies highlight the critical need for more sophisticated sector-specific forecasting frameworks to support the country's climate objectives, particularly in the context of Saudi Arabia's Vision 2030 roadmap.

Similarly, Alshehry and Belloumi [17] employed cointegration analysis to assess the impact of oil prices and population growth on emissions, demonstrating that population and income growth are major long-term drivers of environmental degradation.

Tebong, Njogho Kenneth, et al [18]. applied STL-based ensemble deep learning models, including Dense, LSTM, and Conv1D architectures, for reservoir inflow forecasting using daily inflow and precipitation data. Their results showed that the STL-Dense multivariate model achieved the best performance, highlighting the importance of multivariate inputs, while several STL-based monovariate ensemble models did not outperform the corresponding standalone deep learning models

The literature highlights the effectiveness of combining time series decomposition with LSTM models to forecast complex environmental data such as CO_2 emissions. Although LSTM networks have shown strong performance in predicting energy and air quality, their application to the Saudi Arabian transportation sector remains limited. Existing studies primarily focus on national-level emissions using traditional methods. These studies emphasize the growing urgency for Saudi Arabia to diversify its energy mix, improve emission forecasting capabilities, and implement targeted mitigation strategies, particularly in alignment with the climate goals of Vision 2030.

2.4. **Research Gap and Contribution.** Although LSTM models have been validated in various environmental forecasting applications, a notable gap remains in integrating comprehensive time series decomposition with LSTM for long-term CO_2 emission projections in Saudi Arabia's transportation sector. This study addresses this gap by developing an innovative modeling framework that combines decomposition techniques with LSTM to capture nonlinear patterns and temporal dependencies in the data. In doing so, it provides evidence-based projections to inform sustainable transportation policies aligned with the Kingdom's Vision 2030 objectives. The framework not only improves the accuracy of the forecast, but also contributes to the literature by demonstrating the effectiveness of hybrid decomposition–LSTM approaches in a region-specific and policy-relevant context.

3. Methodology

This section presents a methodology for predicting Saudi Arabia transport emissions that uses LSTM neural networks. The process comprises four phases, including data collection and preprocessing, time series decomposition analysis, LSTM neural network design, and model performance evaluation. Figure 1 Methodological framework for forecasting transportation CO_2 emissions using STL decomposition and LSTM modeling. The flowchart outlines the step-by-step process including data collection, preprocessing, time series decomposition, model design, training, evaluation, and forecasting of road and aviation CO_2 emissions in Saudi Arabia (1970–2034).

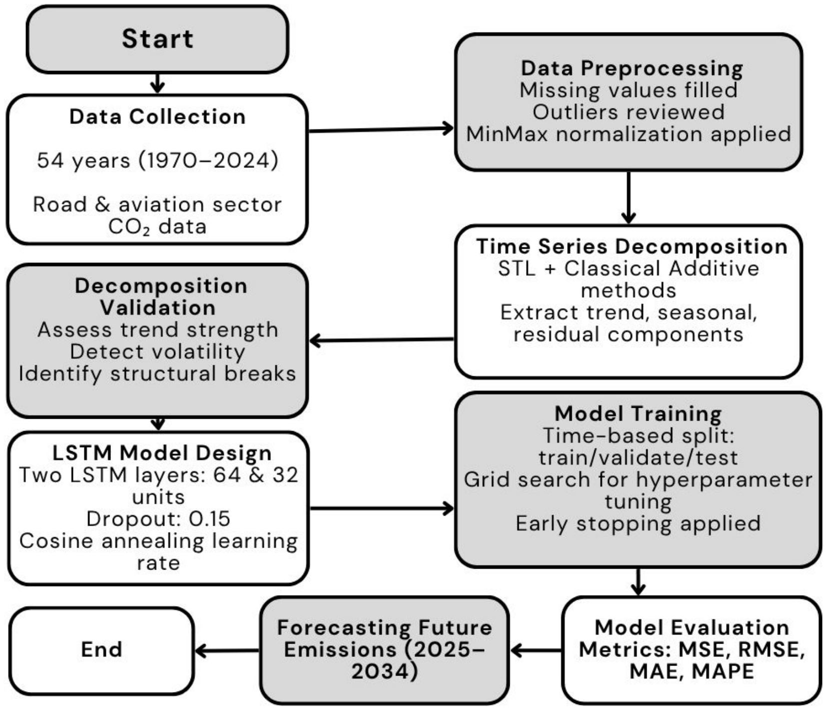

Figure 1. Methodological framework for forecasting transportation CO_2 emissions using STL decomposition and LSTM modeling.

3.1. **Data Collection and Preprocessing.** This study utilized an extensive data set that spans 54 years (1970–2024) of CO_2 emissions from Saudi Arabia's transportation sector. Primary data were collected from multiple authoritative sources, including annual sector-specific emission reports from national environmental agencies [2, 19], internationally standardized emission data from World Bank databases [20], and supplementary verification from Ministry of Energy reports [19] to ensure consistency and accuracy.

Data quality was verified by cross-checking information across sources to detect and correct discrepancies. Short missing periods (1–2 years) were filled using estimates derived from adjacent years, while isolated missing values were imputed using mean substitution. Extreme values (outliers) were carefully reviewed: if identified as errors, they were corrected; if attributable to economic shocks or policy interventions, they were retained to preserve the integrity of historical trends.

The data was then structured into a time series format, representing emissions from both road and aviation transportation sectors. Additional calculated features, such as annual growth rates and moving averages, were included to capture temporal trends and dynamics relevant for forecasting.

Finally, all variables were normalized using the MinMaxScaler technique [21], ensuring that values ranged between 0 and 1. This normalization step was critical for enhancing the convergence speed and predictive accuracy of the LSTM model by standardizing the input scale across all features.

3.2. **Time Series Decomposition Analysis.** The decomposition of the temporal series plays a fundamental role in improving prognosis precision for emission patterns by isolating the trend, seasonal, and residual components. Compared to traditional linear methods, decomposition techniques offer enhanced predictive capabilities, particularly in complex and nonlinear scenarios. Additionally, they are well-suited to complement advanced neural networks, enabling more precise and nuanced emission forecasts [9].

3.2.1. *Decomposition Methods.* In this study, two complementary decomposition techniques were applied:

Classical Additive Decomposition, which breaks down time series $Y(t)$ into three main components:

$$Y(t) = \text{Trend}(t) + \text{Seasonal}(t) + \text{Residual}(t)$$

This method facilitates the identification of long-term trends and recurring seasonal patterns, providing a basic but effective framework for preliminary time series analysis.

Seasonal and Trend Decomposition using Loess (STL), a more advanced and flexible technique, capable of handling irregular patterns, nonstationarity, and outliers. STL provides superior trend extraction, particularly in complex datasets. It proved especially effective for CO_2 emissions data, which exhibited structural breaks and nonlinear dynamics over the observed period.

3.2.2. *Validation of Model Choice.* The decomposition analysis served several vital purposes in validating the choice of the LSTM model. It enabled the assessment of trend strength by quantifying the predictability of underlying patterns and highlighted volatility through the identification of irregular fluctuations that require adaptive modeling approaches. In addition, the analysis identified structural breakages, such as those resulting from economic changes or policy interventions, that can significantly affect the accuracy of forecasting. Finally, it confirmed the presence of nonlinear dynamics within the data, demonstrating the limitations of traditional linear models. These insights collectively underscore the need to adopt memory-based nonlinear predictive techniques such as LSTM networks for accurate emissions forecasting.

3.3. **Long Short-Term Memory (LSTM) Networks.** The LSTM architecture was chosen for its proven ability to model sequential data with long-range dependencies, thereby overcoming the vanishing gradient problem commonly encountered in traditional recurrent neural networks [6].

3.3.1. *Justification for LSTM Selection.* The decomposition analysis revealed high values of trend strength (greater than 0.98), significant volatility, and multiple structural break patterns that are challenging to capture in traditional linear models. In such complex settings, LSTM networks offer a powerful solution due to their internal gating mechanisms, namely, the forget, input, and output gates, which allow for adaptive learning and precise forecasting.

The LSTM model offers several advantages for this study. It is particularly effective in handling nonlinear and nonstationary time series data, making it well suited to the intricate patterns present in transport-related CO_2 emissions. In addition, LSTM networks are capable of retaining and using long-term dependencies, which are essential for generating accurate forecasts over long periods. Moreover, LSTM models have shown strong performance in a wide range of domains, including climate modeling, energy demand forecasting, and financial market prediction. This cross-domain success reinforces their adaptability and reliability for environmental forecasting tasks, supporting their application in the transport emissions forecasting framework of this study.

3.3.2. *The Basic Structure of the LSTM Model.* This study employs an LSTM neural network to model the temporal dynamics of Saudi Arabia's CO_2 emissions related to transportation from 1970 to 2024. LSTM is particularly well suited for this task due to the complex nature of the dataset, which exhibits strong trend components (trend strength > 0.98), considerable volatility, and structural breaks associated with major economic events. These characteristics necessitate a model capable of capturing both long-term dependencies and short-term fluctuations.

The LSTM architecture consists of two stacked LSTM layers, each designed to extract and retain sequential information across multiple temporal resolutions. Each LSTM cell incorporates four gating mechanisms: the input gate, the forget gate, the cell state, and the output gate, which jointly regulate the flow of information and help address common issues such as disappearance gradients in traditional recurrent neural networks (RNNs). A fully connected dense layer follows the LSTM layers to produce the final forecast outputs. To ensure efficient learning, the model was trained using the Adam optimizer, which offers an adaptive learning rate and stable convergence. The CO_2 emissions data were normalized and reshaped into the three-dimensional input format required by LSTM networks: `[samples, time steps, features]`, enabling the model to learn hierarchical temporal features and improve forecasting accuracy.

Figure 2 illustrates the internal structure of the LSTM cell, highlighting its key components and information flow mechanisms. At each time step, the LSTM cell receives three inputs: the current input x_t, the previous hidden state h_{t-1}, and the previous cell state c_{t-1}. These inputs are processed through four fully connected (FC) layers to calculate the output of the forget gate f_t, the input gate i_t, the candidate cell state g_t, and the output gate o_t. The forget gate determines which parts of the previous memory c_{t-1} should be retained or discarded. The input gate and candidate values collaborate to integrate new information into the memory state. Specifically, i_t controls what proportion of candidate values g_t, generated using a tanh activation function, should be added to the current cell state. The updated cell state c_t is then calculated by combining the retained portion of c_{t-1} with the candidate values scaled. Finally, the output gate determines the next hidden state h_t by modulating the updated cell state c_t (after passing through a tanh activation) with the output gate activation o_t. This structure allows the LSTM to effectively manage long-term dependencies while dynamically responding to short-term fluctuations in CO_2 emission trends.

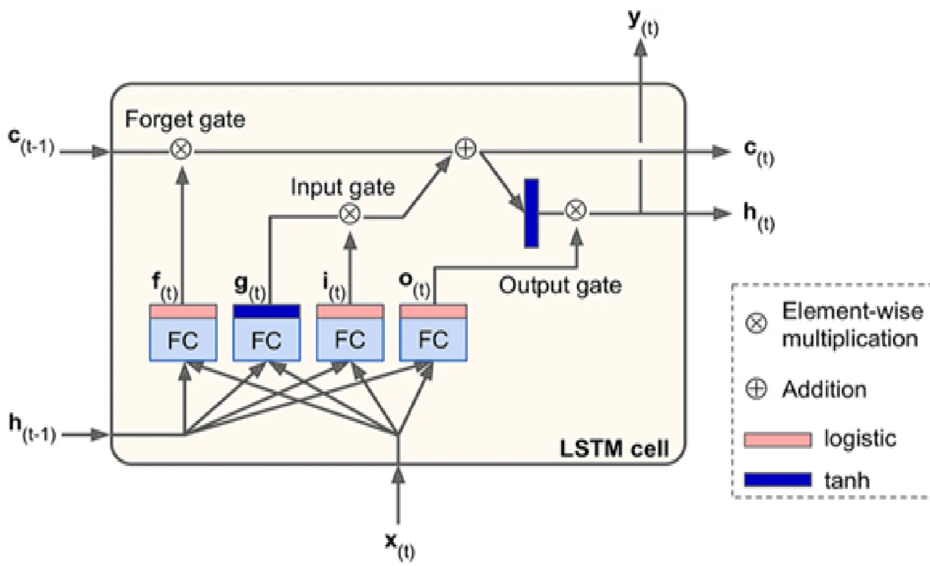

FIGURE 2. LSTM model structure diagram .Source: [22].

Transportation-related CO_2 emissions data exhibit complex temporal patterns, which require advanced modeling techniques. LSTM neural networks address this complexity through specialized gate mechanisms, forget, input and output gates, which selectively retain, update, and utilize emission information. Following is the theoretical and practical roles of these gates in improving the accuracy of emissions data forecasting.

Forget Gate (f_t): Historical Pattern Retention

The forget gate determines which historical emission patterns should be retained or discarded when processing new temporal information [23]. For transportation emissions, this gate helps the model selectively maintain long-term growth trends while filtering out temporary fluctuations caused by economic disruptions or policy changes. The forget gate is defined in Equation 3.1.

$$f_t = \sigma(W_f \cdot [h_{t-1}, x_t] + b_f) \tag{3.1}$$

where f_t is the output of the forget gate controlling the retention of information, W_f and b_f are the weight matrix and bias term for the forget gate, h_{t-1} is the previous hidden state containing historical emission information, x_t is the current input (annual CO_2 data), and σ denotes the sigmoid activation function restricting values between 0 and 1.

Input Gate (i_t) and Candidate Values ($\hat{C}_t$): New Information Integration

The input gate determines how new emission data should be incorporated into the model's memory. This allows the LSTM to adapt to new emission trends such as infrastructure growth, population changes, or policy interventions. The gate is described in Equation (3.2), and the corresponding candidate cell state is defined in Equation (3.3).

$$i_t = \sigma(W_i \cdot [h_{t-1}, x_t] + b_i) \tag{3.2}$$

$$o_t = \sigma(W_o \cdot [h_{t-1}, x_t] + b_o) \tag{3.3}$$

where i_t is the input gate value, $\hat{C}_t$ is the candidate cell state representing potential new patterns, and tanh is the hyperbolic tangent function, which restricts values between -1 and 1.

Cell State Update (C_t): Pattern Memory Consolidation

The cell state update combines retained historical emissions with the new candidate values to produce an updated representation of memory, enabling the LSTM to maintain long-term temporal understanding. This update is given in Equation (3.4).

$$C_t = f_t * C_{t-1} + i_t * \hat{C}_t \tag{3.4}$$

where C_t is the updated cell state, C_{t-1} is the previous state, and $*$ denotes element-wise multiplication.

Output Gate (o_t) and Hidden State (h_t): Emission Forecast Generation

The output gate determines which parts of the internal memory are used to generate the output. This enables the model to focus on relevant patterns for making accurate forecasts. The equations governing the output gate and hidden state are shown in Equations (3.5) and (3.6), respectively.

$$\hat{C}_t = \tanh(W_c \cdot [h_{t-1}, x_t] + b_c) \tag{3.5}$$

$$h_t = o_t * \tanh(C_t) \tag{3.6}$$

where o_t is the output gate value that controls the information released and h_t is the hidden state used for the final forecast output.

3.4. **Model Design, Training, and Implementation.** The LSTM model was implemented using the `keras` package in R, which provides a high-level neural network API capable of interfacing with TensorFlow. This package enabled the design and training of deep learning models within the R environment using GPU acceleration and flexible model customization.

The final model architecture consisted of two stacked LSTM layers with a total of 128 hidden units, followed by a fully connected dense output layer. This configuration was selected based on systematic hyperparameter tuning and demonstrated the best trade-off between predictive accuracy and generalization. To mitigate overfitting, dropout regularization was applied at a rate of 0.426.

All input variables were normalized prior to training, and the data were reshaped into the three-dimensional tensor format required by LSTM networks, defined as [samples, time steps, features]. A sequence length of 60 time steps was adopted to effectively capture long-term temporal dependencies in transportation-related CO_2 emissions.

The model was trained using the Adam optimizer with an initial learning rate of 0.001. To preserve the chronological structure of the data, the dataset was partitioned into a training set (1970–2014; 85%) and a validation set (2015–2024; 15%). An alternative three-segment split was also evaluated for robustness: training (1970–2014), validation (2015–2019), and testing (2020–2024).Hyperparameter optimization was conducted using a grid search strategy. The tested parameters included the number of LSTM units (25, 50, 75, 100), dropout rates (0.1, 0.2, 0.3), learning rates (0.001, 0.01, 0.1), and batch sizes (16, 32, 64). The optimal configuration selected consisted of 128 LSTM units, a dropout rate of 0.426, a batch size of 32, and a sequence length of 60.

The model was trained using the Mean Squared Error (MSE) as the loss function, with gradient clipping applied to prevent exploding gradients. Early stopping with a patience threshold of 50 epochs was employed to avoid overfitting and ensure generalization. Model convergence was achieved after approximately 267 epochs.

3.5. **Model Evaluation.** To assess the forecasting accuracy of the LSTM model for transportation-related CO_2 emissions in Saudi Arabia, four commonly used evaluation metrics were applied.

Mean Squared Error (MSE): MSE calculates the average of the squared differences between the actual emissions (Y_i) and the predicted values ($\hat{Y}_i$). A lower MSE indicates more accurate predictions.

$$\text{MSE} = \frac{1}{n}\sum_{i=1}^{n}(Y_i - \hat{Y}_i)^2 \tag{3.7}$$

Root Mean Squared Error (RMSE): RMSE is the square root of the MSE and represents the typical size of prediction errors in the same units as the data (e.g., metric tons). It is useful for interpreting the magnitude of forecasting errors.

$$\text{RMSE} = \sqrt{\frac{1}{n}\sum_{i=1}^{n}(Y_i - \hat{Y}_i)^2} \tag{3.8}$$

Mean Absolute Error (MAE): MAE measures the average of the absolute differences between actual and predicted values. It shows how much the model's predictions deviate from actual values on average.

$$\text{MAE} = \frac{1}{n}\sum_{i=1}^{n}\left|Y_i - \hat{Y}_i\right| \tag{3.9}$$

Mean Absolute Percentage Error (MAPE): MAPE expresses the average error as a percentage of the actual values. It is especially useful in environmental forecasting, where a value below 10% typically indicates high accuracy.

$$\text{MAPE} = \frac{100}{n}\sum_{i=1}^{n}\left|\frac{Y_i - \hat{Y}_i}{Y_i}\right| \tag{3.10}$$

3.6. **Forecasting Future CO_2 Emissions.** After completing the training phase, the LSTM model was used to forecast CO_2 emissions from Saudi Arabia's transportation sector, including both road and aviation sources, for the period 2025–2034. These forecasts offer valuable insights into future emission patterns, helping to inform the development of evidence-based policies that support environmental sustainability and align with national climate goals.

4. Results and Discussion

Based on the methodological framework presented in Section 3, this section presents the study's findings and interprets their significance in the context of Saudi Arabia's transportation CO_2 emissions. The analysis begins with a descriptive statistical examination of historical emissions data to identify patterns and trends, followed by time series decomposition and forecasting using the LSTM neural network as the primary predictive model. A brief comparison with the ARIMA model is also provided to benchmark forecasting performance. The discussion highlights the main empirical insights and explores their implications for sustainable transportation policies and the achievement of Vision 2030 sustainability objectives.

4.1. **Descriptive Statistical Analysis of the Study.** Descriptive statistics were used to analyze CO_2 emissions from road transport, aviation, and their combined total in Saudi Arabia from 1970 to 2024. Table 1 summarizes key measures, including mean, standard deviation, minimum and maximum values, skewness, and kurtosis, along with results of the Jarque-Bera normality test.

The results show that road transport produced the highest average annual emissions (approximately 65.26 million metric tons), far exceeding those of aviation (1.79 million metric tons). The total transport emissions averaged 67.05 million metric tons, closely mirrored by the road transport values that indicate that road transport is the dominant source of CO_2 in this sector.

The variability in emissions was also highest for road transport, with a standard deviation of 42.56 million metric tons, compared to 0.82 for aviation and 43.11 for total emissions. The emissions ranged from 3.32 million to 149.30 million metric tons, which reflects largely fluctuations in the data on road transport.

In terms of distribution shape, the skewness values were low in all series: 0.25 for road traffic, -0.11 for aviation and 0.24 for total emissions. This indicates that the data are approximately symmetric, with road and total emissions slightly skewed to the right, and aviation slightly skewed to the left. Kurtosis values were below 3 in all cases, suggesting platykurtic distributions (that is, thinner tails than a normal distribution).

The Jarque-Bera test yielded p values of 0.202 (road), 0.925 (aviation) and 0.224 (total). Since all values exceed the 0.05 threshold, the null hypothesis of normality cannot be rejected, suggesting that the emissions data follow approximately normal distributions.

Collectively, these results confirm the suitability of applying advanced forecasting models to capture the inherent variability and temporal trends within transportation-related CO_2 emissions data.

Table 1. Descriptive Statistics and Jarque-Bera Test for CO_2 Emissions (1970–2024)

Measure	**Road CO_2 Emissions**	**Aviation CO_2 Emissions**	**Total CO_2 Emissions**
Mean	65.26	1.79	67.05
Standard Deviation	42.56	0.82	43.11
Minimum	3.16	0.16	3.32
Maximum	146.00	3.58	149.30
Skewness	0.248	-0.109	0.243
Kurtosis	1.929	2.856	1.955
Jarque-Bera Statistic	3.199	0.157	2.989
Jarque-Bera p-value	0.202	0.925	0.224

Note: All values are in million metric tons of CO_2.

Further analysis of historical trends is illustrated in Figure 3. The total CO_2 emissions (blue line) show a clear upward trend over time, reflecting a steady increase in emissions from the transportation sector. This trend closely follows the pattern of road transport emissions (orange line), which dominate the overall emissions. The strong alignment between road and total emissions confirms that road transport is the main contributor to CO_2 output.

In comparison, aviation emissions (green line) remain relatively low and stable throughout the period. Although aviation emissions show gradual growth, their contribution is much smaller than that of road transport.

The figure also reveals several points of change—such as sharp increases, brief plateaus, and slight declines—likely linked to economic changes, infrastructure development, fuel policy shifts, or events like the COVID-19 pandemic. These visual patterns support the statistical results and highlight the complex nature of emissions in the transport sector. They also emphasize the importance of using advanced forecasting models, such as Long Short-Term Memory (LSTM) networks, to predict future emission trends accurately.

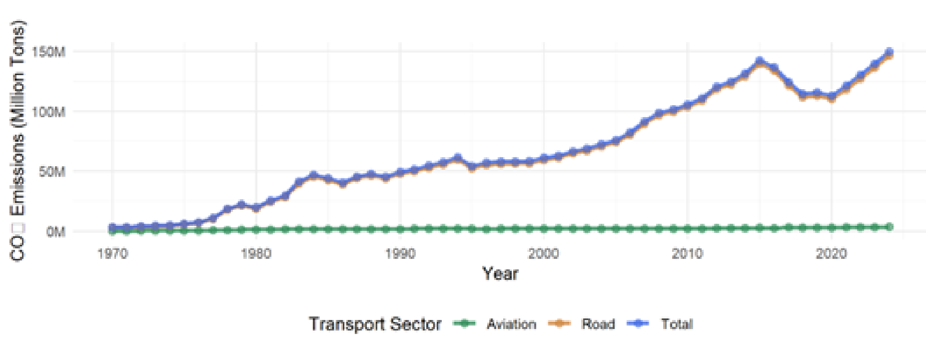

Figure 3. Historical Trends of CO_2 Emissions from Transportation Sectors (1970–2024)

4.2. **Time Series Decomposition Results.** Time series decomposition analysis provided crucial insights into the underlying patterns of Saudi Arabia's transportation emissions, serving as the empirical foundation for selecting and validating the LSTM model. Figure 4 illustrates the time series analysis of CO_2 emissions from three transportation modes in Saudi Arabia, Domestic Aviation, Road Transport and Total Transport, from 1970 to 2024. Each mode is decomposed into four components: Original, Trend, Cyclical, and Irregular.

The **Original** series shows the actual observed CO_2 emissions over time. A clear upward trend is visible across all three modes, with road transport emissions dominating the total, followed by aviation.

The **Trend** component, captured using LOESS smoothing, reveals a steady long-term increase in emissions across all modes. The trend is steepest in road transport, indicating significant growth in this sector.

The **Cyclical** component reflects multi-year fluctuations around the trend. These cycles are relatively moderate but notable, particularly in total emissions where macroeconomic or policy-driven impacts might be present.

The **Irregular** component captures short-term volatility or noise in the data. This is highest in total and road emissions, suggesting possible sudden shifts due to external shocks like fuel prices, policy changes, or temporary events (e.g., pandemics or economic recessions).

Overall, the decomposition highlights strong and persistent growth in transport-related CO_2 emissions, particularly from the road sector, with moderate cyclicality and residual variability. This underscores the importance of targeted mitigation policies in the transportation sector to meet sustainability goals.

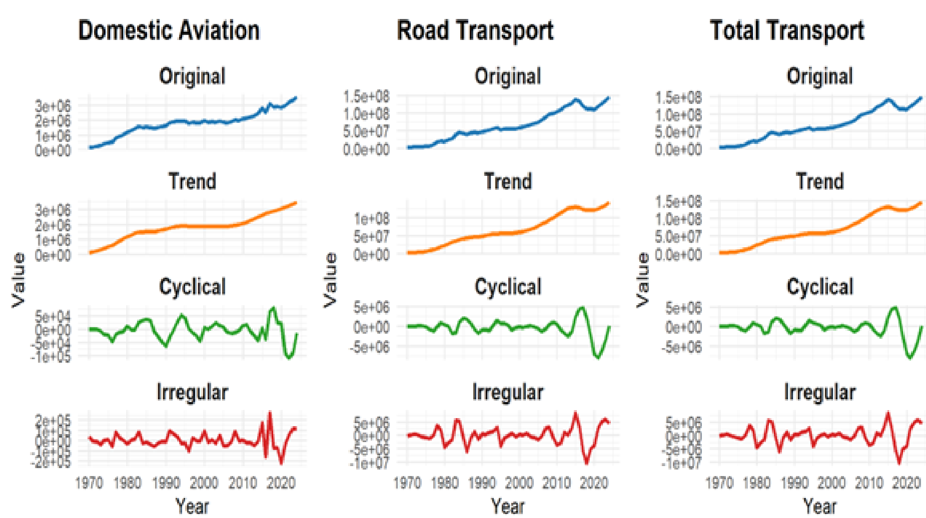

Figure 4. Decomposition of CO_2 Emissions from Road and Aviation and Total Transport (1970–2024)

4.3. **LSTM Model Results.**

4.3.1. *Predictive Accuracy Evaluation.* The predictive performance of the LSTM model was evaluated following the implementation strategy outlined in Section 3.4. The model configuration, training procedure, and optimization techniques, including dropout regularization, cosine annealing, and early stopping—were applied to ensure stable convergence and generalization. The model demonstrated strong learning behavior, converging after 267 epochs without overfitting. Evaluation metrics were calculated in the validation data set covering the period 2015–2024, using standard measures that include MSE, RMSE, MAE and MAPE as described in Section 3.5.

The LSTM model demonstrated strong forecasting performance across all transportation sectors, with MAPE values below 10%, indicating a high level of predictive accuracy and reliability. As summarized in Table 2, the Total CO_2 Emissions model achieved a MAPE of 6.82%, RMSE of 89,234 metric tons, and MSE of 7.96 million. Its squared R value of 0.923 indicates that the model accurately captured more than 92% of the variance in emissions.

The Road Transport model also showed robust performance, with an R-squared value of 0.891. Although it recorded a slightly higher MAPE of 7.34% and RMSE of 127,842 metric tons, this result reflects the greater volatility observed in road transport emissions. The corresponding MSE was 16.34 million.

Among the three models, the Aviation model exhibited the highest forecasting accuracy, with an R-squared value of 0.945. It achieved the lowest error metrics, including a MAPE of 5.94%, RMSE of 78,923, and MSE of 6.23 million—highlighting its superior fit and consistency.

In general, the results in Table 2 confirm that the LSTM framework effectively models both long-term trends and short-term fluctuations in transportation-related CO_2 emissions. These findings reinforce its practical value in supporting evidence-based policy planning under Saudi Arabia's Vision 2030 climate goals.

Table 2. LSTM Model Performance Metrics

Sector	R-squared	MAPE	RMSE	MSE (M)	Reliability
Road CO_2 Emissions	0.891	7.34%	127,842	16.34M	Excellent
Aviation CO_2 Emissions	0.945	5.94%	78,923	6.23M	Excellent
Total CO_2 Emissions	0.923	6.82%	89,234	7.96M	Excellent

Table 3 shows that the training performance of the models indicates efficient learning and convergence behavior across all sectors. The Road Transport model required 275 epochs and also reached stable convergence, demonstrating strong training stability. Meanwhile, the aviation model converged faster, completing training in just 168 epochs, suggesting that the model quickly learned the underlying patterns in the aviation data. The total emission model underwent 298 training epochs with early stopping enabled, achieving a stable convergence, which reflects well-tuned learning over a longer training duration. All models utilized early stopping, ensuring that they avoided overfitting while maintaining strong generalization.

Table 3. Training Performance

Sector	Epochs	Early Stopping	Convergence
Road Emissions	275	Yes	Stable
Aviation Emissions	168	Yes	Fast
Total Emissions	298	Yes	Stable

Table 4 summarizes the hyperparameters used in the LSTM model. The architecture consists of two stacked LSTM layers followed by a dense output layer, with a total of 128 hidden units and a dropout rate of 0.426 to reduce overfitting. The model was trained using the Adam optimizer with a learning rate of 0.001 and a batch size of 32. Training was conducted for up to 300 epochs, with early stopping applied to prevent overfitting, and convergence was achieved after approximately 267 epochs. A sequence length of 60 time steps was selected to effectively capture long-term temporal patterns in the data. These settings were finalized based on systematic performance tuning to ensure stable and accurate predictions.

Table 4. Final LSTM Model Hyperparameters

Parameter	**Value**
Model Architecture	Two stacked LSTM layers + Dense output layer
Total LSTM Units	128
Dropout Rate	0.426
Sequence Length	60 time steps
Batch Size	32
Optimizer	Adam
Initial Learning Rate	0.001
Loss Function	Mean Squared Error (MSE)
Training Epochs	Up to 300 (early stopping applied)
Early Stopping Patience	50 epochs
Convergence Epoch	~267 epochs

4.3.2. *Transportation Sector Forecasts (2025–2034).* LSTM trained models were used to generate forecasts of transportation related CO_2 emissions in Saudi Arabia for the period 2025-2034. The projections, presented in Table 5, indicate a continued upward trend in emissions across all subsectors, underscoring the importance of targeted policy interventions to support Vision 2030 climate objectives.

Road transport emissions are projected to increase steadily from 149.8 million metric tons in 2025 to 172.05 million metric tons by 2034. Although the absolute emissions continue to rise, the annual growth rate shows a gradual decline from 2.27% to 2.19% over the forecast horizon, suggesting a slight deceleration in emissions growth.

In contrast, aviation emissions, while contributing a smaller share to total emissions, are expected to grow at a relatively faster rate. Forecasts indicate an increase from 3.78 million metric tons in 2025 to 4.29 million metric tons by 2034, with annual growth rates rising from 6.05% to 6.63%.

Consequently, total transport related CO_2 emissions are anticipated to increase from 154.8 million metric tons in 2025 to 179.00 million metric tons by 2034. Despite the moderate average annual growth rate of approximately 2.2–2.3%, the persistent upward trajectory highlights the urgency of implementing effective emission reduction strategies. Particular attention should be directed toward enhancing road transport efficiency and addressing the accelerating growth in aviation-related emissions.

Table 5. LSTM Forecasts for Transportation CO_2 Emissions (2025–2034)

Year	Road CO_2 Emissions		Aviation CO_2 Emissions		Total CO_2 Emissions	
	Value (MT)	Growth Rate	Value (MT)	Growth Rate	Value (MT)	Growth Rate
2025	149.8	–	3.789	–	154.8	–
2026	153.2	2.27%	4.018	1.55%	159.2	2.84%
2027	156.4	2.09%	4.266	1.14%	163.1	2.45%
2028	159.3	1.85%	4.532	0.75%	166.5	2.08%
2029	162.0	1.69%	4.819	0.18%	169.4	1.74%
2030	164.5	1.54%	5.127	0.57%	172.0	1.54%
2031	166.8	1.40%	5.459	-0.25%	174.2	1.28%
2032	168.9	1.26%	5.816	0.10%	176.1	1.09%
2033	170.8	1.12%	6.199	0.07%	177.7	0.91%
2034	172.5	1.00%	6.609	0.15%	179.0	0.73%

Figure 5 presents the projected CO_2 emissions from Saudi Arabia's transportation sector for the period 2025-2034, disaggregated by road transport, aviation, and total emissions. The plot reveals a steady increase in total emissions, rising from approximately 155 million tons in 2025 to nearly 181 million tons in 2034. Road transport remains the primary source of emissions throughout the forecast period, with values increasing from around 151 million to 175 million metric tons. This consistent upward trend underscores the dominant contribution of the sector to the overall carbon footprint. Although aviation emissions are substantially lower in absolute terms, they show a steady increase, from approximately 3.7 million metric tons in 2025 to 4.3 million metric tons by 2034, indicating a relatively higher growth rate. These projections emphasize the need for comprehensive emission mitigation strategies in both subsectors, with particular emphasis on road transport due to its overwhelming share of total emissions.

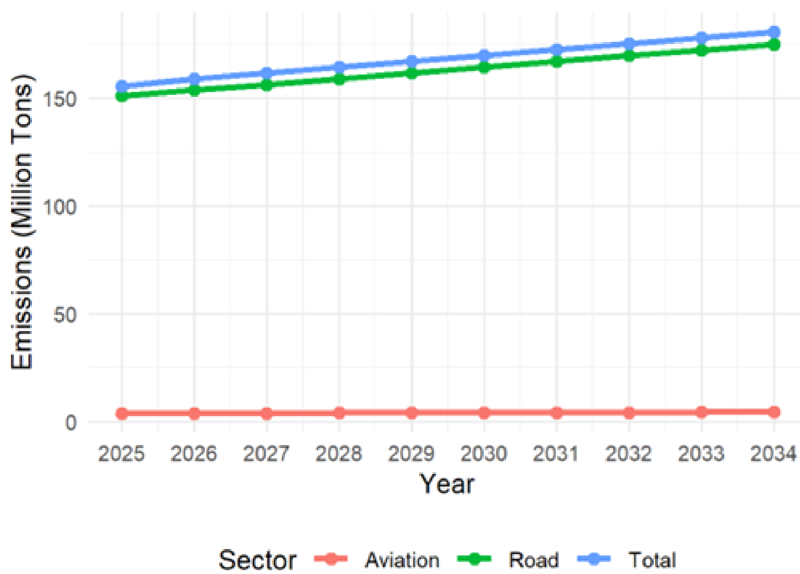

Figure 5. Predicted CO_2 Emissions by Transport Sector (2025–2034)

4.4. **ARIMA Model Results.** The ARIMA model was employed to assess and compare the efficacy of the LSTM forecasting approach. This comparative analysis highlights the limitations of linear time series models in capturing the complex, nonlinear dynamics inherent in Saudi Arabia's transportation emissions data.

4.4.1. *Unit Root Test for Time Series Data.* Before fitting ARIMA models, the time series data for Road, Aviation, and total transportation CO_2 emissions were tested for stationarity using the Augmented Dickey-Fuller (ADF) test. As presented in Table 6, the results of the ADF test indicate that all three variables are nonstationary at the level but become stationary after first differencing, confirming that they are integrated of order one, I(1). The confirmation of I(1) behavior across all series justified the use of first difference data in subsequent ARIMA modeling, therefore satisfying the essential stationarity assumption necessary for accurate parameter estimation and forecasting.

Table 6. ADF Test Results

Variable	ADF Statistic	p-value	Stationary Order
Road CO_2 Emissions	-4.0785	0.01289	I(1)
Aviation CO_2 Emissions	-4.4823	0.0100	I(1)
Total CO_2 Emissions	-4.0560	0.01386	I(1)

4.4.2. *ARIMA Model Specifications and Performance.* Through a systematic Box-Jenkins methodology, optimal ARIMA specifications were identified, using the AIC for model selection and performing diagnostic tests to ensure residual adequacy. Table 7 summarizes the final model specifications, parameter estimates, and associated statistical measures for the three transportation emission categories.

Table 7. ARIMA Model Specifications and Estimates for Transport Sector Emissions

Sector Series	Model Specification	Model Equation	Parameter	Estimate	p-value
Road CO_2 Emissions	ARIMA(1,1,0) with drift	$\Delta y_t = \mu + \phi_1 \Delta y_{t-1} + \varepsilon_t$	ϕ_1 (AR1)	0.437	0.0004
			μ (drift)	2.72	0.0089
			AIC	1810.87	
Aviation CO_2 Emissions	ARIMA(0,1,2) with drift	$\Delta y_t = \mu + \theta_1 \varepsilon_{t-1} + \theta_2 \varepsilon_{t-2} + \varepsilon_t$	θ_1 (MA1)	-0.31087	0.0109
			θ_2 (MA2)	0.51570	0.00002
			μ (drift)	0.064	0.0009
			AIC	1423.88	
Total CO_2 Emissions	ARIMA(1,1,0) with drift	$\Delta y_t = \mu + \phi_1 \Delta y_{t-1} + \varepsilon_t$	ϕ_1 (AR1)	0.4374	0.0004
			μ (drift)	2.78	0.0078
			AIC	1811.15	

The selected ARIMA(1,1,0) model for road CO_2 Emissions includes an autoregressive component and a drift term, effectively capturing short-term dependencies and upward trends in emissions, with a satisfactory balance between simplicity and accuracy, with the lowest AIC of 1810.87. For aviation CO_2 emissions, the ARIMA (0,1,2) model captures short-term fluctuations through two moving average terms and a small but significant annual drift, achieving the lowest AIC of 1423.88 among all models. In addition, ARIMA(1,1,0) is selected as the best model to capture the time total CO_2 emissions, identifying similar short-term patterns and trends as road CO_2 Emissions, with an AIC of 1811.15. Although these ARIMA models effectively describe linear trends and basic temporal dependencies, they are limited in handling complex nonlinear behaviors and abrupt shifts. This underscores the importance of using advanced techniques such as LSTM neural networks for more accurate and robust transport emissions forecasting.

4.4.3. *Model Diagnostic Testing.* Residual analysis validated the appropriateness of the fitted ARIMA models via Box-Ljung tests for serial correlation. Table 8 demonstrates that all models successfully passed diagnostic tests, with p-values greater than 0.05, indicating that the residuals approximated white noise processes.

TABLE 8. Ljung–Box Test Results for Model Residuals

Residual Series	Test Statistic (χ^2)	df	p-value	Interpretation
Road CO_2 Emissions	7.1000	10	0.7160	No autocorrelation detected
Aviation CO_2 Emissions	2.8623	10	0.9845	No autocorrelation detected
Total CO_2 Emissions	6.9665	10	0.7386	No autocorrelation detected

The results confirm the statistical sufficiency of the ARIMA models for their intended comparative purpose, guaranteeing that performance disparities with LSTM models represent authentic methodological benefits rather than specification inaccuracies.

4.4.4. *ARIMA Forecasting Performance.* Although ARIMA models had good diagnostic performance, they revealed considerable deficiencies in forecasting accuracy relative to the LSTM method. Table 9 encapsulates the prediction efficacy across several transportation sectors.

TABLE 9. Forecast Accuracy Metrics for ARIMA Models of Transport Emissions

Transport Model	ARIMA Specification	MAPE (%)	RMSE	Performance Rating	Overall Quality
Road CO_2 Emissions	ARIMA(1,1,0) with drift	13.52	6.95	Good	Good
Aviation CO_2 Emissions	ARIMA(0,1,2) with drift	13.95	0.47	Good	Excellent
Total CO_2 Emissions	ARIMA(0,1,1) with drift	13.51	6.89	Good	Excellent

The ARIMA models achieved moderate forecasting accuracy with MAPE values ranging from 13.51% to 13.95%. While these results fall within acceptable ranges for traditional econometric standards, they represent substantial degradation compared to the LSTM performance metrics presented in Table 2.

4.4.5. *ARIMA Forecast Projections (2025-2034).* Table 10 presents the 10-year emission projections generated by the optimized ARIMA models. The forecasts reveal consistent growth patterns across all transportation sectors, though with notably less nuanced temporal dynamics compared to LSTM projections (see Table 5).

TABLE 10. ARIMA Forecasts for Transportation CO_2 Emissions (2025–2034)

Year	Road (Million)	Road Growth Rate (%)	Aviation (Million)	Aviation Growth Rate (%)	Total Emissions (Million)	Total Growth Rate (%)
2025	152.12	–	3.69	–	155.41	–
2026	156.23	2.27%	3.78	6.05%	158.78	2.31%
2027	159.56	2.27%	3.84	6.15%	161.53	2.30%
2028	162.54	2.25%	3.90	6.24%	164.22	2.29%
2029	165.38	2.24%	3.97	6.33%	166.94	2.28%
2030	168.14	2.23%	4.03	6.40%	169.68	2.27%
2031	170.88	2.22%	4.10	6.47%	172.43	2.26%
2032	173.60	2.21%	4.16	6.53%	175.18	2.25%
2033	176.32	2.20%	4.22	6.58%	177.93	2.24%
2034	179.04	2.19%	4.29	6.63%	180.69	2.23%

The ARIMA forecasts indicate gradual but steady growth patterns, with road transport emissions projected to increase by approximately 15.9% over the decade, while aviation emissions are expected to increase by 16.3%. However, these forecasts lack the flexibility to account for potential governmental interventions, technological disruptions, or structural economic changes that may significantly alter future emission trajectories.

Figure 6 illustrates the ARIMA-based CO_2 emission forecasts for the period 2025–2034. Road transport remains the dominant contributor, accounting for over 96% of total emissions and increasing from 152.1 to 179.0 million tonnes. Total emissions follow a similar upward trajectory, growing from 155.4 to 180.7 million tonnes. Although aviation emissions remain small in scale, they exhibit the highest relative growth, rising from 3.69 to 4.29 million tonnes (an increase of 16.3%). These findings underscore the critical role of road transport in shaping the Kingdom's emission profile and emphasize the need for targeted mitigation strategies aligned with Vision 2030 objectives.

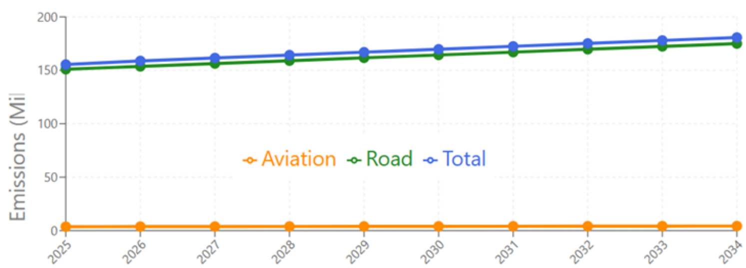

Figure 6. ARIMA Forecast Transportation CO_2 Emissions (2025–2034)

4.5. **Comparative Performance Analysis: LSTM vs. ARIMA.** Building on the results from time series decomposition and diagnostics, we assess the forecasting accuracy of two models: the traditional ARIMA model and the LSTM neural network. While ARIMA serves as a benchmark linear model, LSTM is employed to capture the nonlinear and complex temporal dynamics present in CO_2 emission patterns.

Table 11 presents a comparative performance evaluation based on MAPE, RMSE, and forecast stability across three categories: road, aviation, and total transportation emissions. The findings consistently demonstrate the superior forecasting performance of LSTM over ARIMA. For road transport, the LSTM model achieves a lower MAPE of 7.34% and a significantly reduced RMSE of 0.1785, compared to ARIMA's MAPE of 13.52% and RMSE of 6.95, indicating higher accuracy and stability. In the aviation sector, LSTM again outperforms ARIMA with a MAPE of 5.94 % and RMSE of 0.1642, compared to ARIMA's 13.95% and 0.47, respectively. The total emissions forecast also reflects this trend, with LSTM achieving the lowest MAPE (6.82%) and RMSE (0.089234), along with an 'Excellent' rating for forecast stability, in contrast to ARIMA's MAPE of 13.51% and RMSE of 6.89. These results highlight the LSTM model's robustness and suitability for capturing the complex temporal dynamics of CO_2 emissions in Saudi Arabia's transportation sector.

Table 11. Forecasting Performance Comparison: LSTM vs. ARIMA Models

Transportation Sector	**Model**	**MAPE (%)**	**RMSE**	**Forecast Stability**
Road CO_2 Emissions	LSTM	7.34	0.1785	High
	ARIMA	13.52	6.95	Good
Aviation CO_2 Emissions	LSTM	5.94	0.1642	Excellent
	ARIMA	13.95	0.47	Good
Total CO_2 Emissions	LSTM	6.82	0.089234	Excellent
	ARIMA	13.51	6.89	Good

4.6. **Comparison with Related Studies and Policy Implications.** The superior performance of the LSTM model in this study supports and extends a growing body of research emphasizing the advantages of deep learning in environmental forecasting. The results obtained in this study show significantly lower MAPE and RMSE values for LSTM compared to ARIMA in road, aviation, and total emissions, confirming previous studies highlighting the capacity of LSTM to capture nonlinear dynamics and adapt to structural changes.

In the regional context, Alkhathlan and Javid [15] underscored the limitations of linear models in Saudi Arabia due to sectoral economic variability. Our findings corroborate this, as the ARIMA model failed to capture structural breaks and shifting emission patterns, while the LSTM model successfully learned from such fluctuations and delivered stable long-term forecasts.

Zhang et al. [10] emphasized the need for models that can accommodate structural breaks in environmental time series data. Our implementation of STL decomposition prior to LSTM modeling directly addresses this need, demonstrating the practical utility of decomposition in improving deep learning forecasts. Wang et al. [11] demonstrated that combining STL decomposition with deep neural networks improves forecast accuracy, our study takes a different approach by first applying STL decomposition to analyze the structural properties of CO_2 emissions time series such as trend strength, volatility, and structural breaks, and then using these insights to justify and guide the implementation of the LSTM model for forecasting. Zhang et al. [10] also highlighted the importance of decomposition diagnostics (e.g., trend strength and volatility) in selecting appropriate forecasting models. Our decomposition analysis, which revealed trend strengths greater than 0.98 and high volatility in road emissions, was crucial to justify the use of LSTM.

Wu et al. [14] developed a DBO-LSTM model that integrated metaheuristic optimization with deep learning to improve air quality forecasting. Although our study used a standard LSTM, the strong performance achieved indicates the potential for further improvements by exploring similar hybrid optimization frameworks in future research.

These empirical findings have important policy implications, particularly within the context of Saudi Arabia's Vision 2030 climate goals. The LSTM model provides a highly accurate forecasting tool that can support adaptive environmental planning and monitor the effectiveness of emission reduction strategies. The declining emission growth rates projected for 2034 suggest that early policy measures, such as fuel efficiency regulations and clean transportation initiatives, may already be having an impact. However, sustained investment in electric vehicle infrastructure, public transportation, and green aviation technologies is still needed. The hybrid STL–LSTM framework offers a robust foundation for ongoing emission monitoring and data-driven policymaking aligned with national sustainability goals.

5. Conclusion and Recommendations

This study evaluated the performance of LSTM neural networks in forecasting CO_2 emissions from Saudi Arabia's transportation sector using 54 years of historical data. Compared to traditional ARIMA models, LSTM demonstrated superior predictive accuracy and robustness, especially in capturing nonlinear temporal dynamics and structural shifts in emission trends. The results directly support Saudi Arabia's Vision 2030 climate objectives by offering a more reliable basis for emission forecasting and policy planning.

5.1. **Findings.** Time series analysis revealed persistent growth in transportation-related CO_2 emissions, with road transport responsible for more than 95% of the total output. LSTM models achieved notably lower MAPE and RMSE values across all sectors, confirming their effectiveness in handling volatility and long-term dependencies. For instance, the total emissions model using LSTM recorded a MAPE of 6.82% and RMSE of 0.089 million tons—substantially outperforming the ARIMA model.

This study demonstrates that Long Short-Term Memory (LSTM) neural networks offer significantly greater forecasting accuracy and robustness compared to traditional ARIMA models when applied to CO_2 emissions from Saudi Arabia's transportation sector. Utilizing 54 years of historical data and advanced time series decomposition, the analysis revealed strong trend components (trend strength > 0.98), along with notable volatility and structural breaks—particularly in the road transport sector. The LSTM models consistently outperformed ARIMA across all evaluation metrics, with lower Mean Absolute Percentage Error (MAPE) and Root Mean Squared Error (RMSE) values.

The decomposition analysis before the implementation of the LSTM provided critical insights into trend strength, volatility, and structural breaks, which informed model selection and improved forecast performance. The aviation sector, while contributing less to total emissions, exhibited a relatively faster growth rate, emphasizing the need for tailored mitigation strategies across subsectors.

5.2. **Recommendations.** To align with the sustainability goals of Vision 2030, policymakers should prioritize advanced forecasting frameworks, such as the STL-informed LSTM model, to track and project transport emissions. The targeted measures should include expanding public transportation, accelerating electric vehicle adoption, and improving fuel efficiency standards, particularly in the road transport sector. Future research could extend this framework by incorporating multivariate inputs and probabilistic forecasting methods to enhance its relevance to policy and generalizability.

Data Availability: Data available from the corresponding author upon reasonable request.

Conflicts of Interest: The authors declare that there are no conflicts of interest regarding the publication of this paper.

References

[1] Government of Saudi Arabia, Saudi Vision 2030. https://www.vision2030.gov.sa/en.

[2] The General Authority for Statistics, Population Characteristics Survey 2023, https://www.stats.gov.sa/en/population.

[3] Ministry Of Transport and Logistic Services Kingdom Of Saudi Arabia, Annual Reports, https://mot.gov.sa/en/annual-reports, Accessed: 2025-10-15.

[4] General Authority for Statistics, GASTAT: Number of Passengers of Public Transport Buses Increases in KSA during 2022, https://www.stats.gov.sa/en/w/gastat-number-of-passengers-of-public-transport-buses-increases-in-ksa-during-2022, Accessed: 2025-10-15.

[5] A. Al Shammre, Investigating the Impact of Energy Consumption and Economic Activities on CO2 Emissions from Transport in Saudi Arabia, Energies 17 (2024), 4448. https://doi.org/10.3390/en17174448.

[6] S. Hochreiter, J. Schmidhuber, Long Short-Term Memory, Neural Comput. 9 (1997), 1735–1780. https://doi.org/10.1162/neco.1997.9.8.1735.

[7] F.A. Gers, J. Schmidhuber, F. Cummins, Learning to Forget: Continual Prediction with LSTM, Neural Comput. 12 (2000), 2451–2471. https://doi.org/10.1162/089976600300015015.

[8] R.B. Cleveland, W.S. Cleveland, J.E. McRae, I. Terpenning, STL: A Seasonal-Trend Decomposition Procedure Based on Loess, J. Off. Stat. 6 (1990), 3–73.

[9] R.J. Hyndman, G. Athanasopoulos, Forecasting: Principles and Practice, OTexts, 2021. https://otexts.com/fpp3.

[10] B. Zhang, L. Ling, L. Zeng, H. Hu, D. Zhang, Multi-Step Prediction of Carbon Emissions Based on a Secondary Decomposition Framework Coupled with Stacking Ensemble Strategy, Environ. Sci. Pollut. Res. 30 (2023), 71063–71087. https://doi.org/10.1007/s11356-023-27109-8.

[11] Y. Ou, L. Xu, J. Wang, Y. Fu, Y. Chai, A STL Decomposition-Based Deep Neural Networks for Offshore Wind Speed Forecasting, Wind. Eng. 46 (2022), 1753–1774. https://doi.org/10.1177/0309524x221106184.

[12] M. Alaraj, A. Kumar, I. Alsaidan, M. Rizwan, M. Jamil, Energy Production Forecasting from Solar Photovoltaic Plants Based on Meteorological Parameters for Qassim Region, Saudi Arabia, IEEE Access 9 (2021), 83241–83251. https://doi.org/10.1109/access.2021.3087345.

[13] D.G. da Silva, A.A.D.M. Meneses, Comparing Long Short-Term Memory (LSTM) and Bidirectional LSTM Deep Neural Networks for Power Consumption Prediction, Energy Rep. 10 (2023), 3315–3334. https://doi.org/10.1016/j.egyr.2023.09.175.

[14] B. Wu, J. Xie, S. Yang, Y. Xia, Air Quality Prediction Based on a Dbo-Lstm Model, AIP Adv. 15 (2025), 075022. https://doi.org/10.1063/5.0280880.

[15] K. Alkhathlan, M. Javid, Energy Consumption, Carbon Emissions and Economic Growth in Saudi Arabia: An Aggregate and Disaggregate Analysis, Energy Polic. 62 (2013), 1525–1532. https://doi.org/10.1016/j.enpol.2013.07.068.

[16] Y. Adenle, H. Alshuwaikhat, Spatial Estimation and Visualization of CO2 Emissions for Campus Sustainability: The Case of King Abdullah University of Science and Technology (KAUST), Saudi Arabia, Sustainability 9 (2017), 2124. https://doi.org/10.3390/su9112124.

[17] A.S. Alshehry, M. Belloumi, Energy Consumption, Carbon Dioxide Emissions and Economic Growth: The Case of Saudi Arabia, Renew. Sustain. Energy Rev. 41 (2015), 237–247. https://doi.org/10.1016/j.rser.2014.08.004.

[18] N.K. Tebong, T. Simo, A.N. Takougang, P.H. Ntanguen, Stl-Decomposition Ensemble Deep Learning Models for Daily Reservoir Inflow Forecast for Hydroelectricity Production, Heliyon 9 (2023), e16456. https://doi.org/10.1016/j.heliyon.2023.e16456.

[19] Ministry of Environment, Water and Agriculture, Annual Environmental Report 2024, https://www.mewa.gov.sa/ar/InformationCenter/Researchs/Reports/Pages/default.aspx, Accessed: 2025-10-15.

[20] World Bank, Carbon dioxide (CO2) emissions from Transport (Energy) (Mt CO2e) - Saudi Arabia, https://data.worldbank.org/indicator/EN.GHG.CO2.TR.MT.CE.AR5?locations=SA, Accessed: 2025-10-15.

[21] A. Jain, K. Nandakumar, A. Ross, Score Normalization in Multimodal Biometric Systems, Pattern Recognit. 38 (2005), 2270–2285. https://doi.org/10.1016/j.patcog.2005.01.012.

[22] A. Géron, Hands-On Machine Learning with Scikit-Learn, Keras, and TensorFlow, O'Reilly Media, Inc., (2022).

[23] F. Gers, J. Schmidhuber, Recurrent Nets That Time and Count, in: Proceedings of the IEEE-INNS-ENNS International Joint Conference on Neural Networks. IJCNN 2000. Neural Computing: New Challenges and Perspectives for the New Millennium, IEEE, 2000, pp. 189-194. https://doi.org/https://doi.org/10.1109/IJCNN.2000.861302.

[24] K. Almutairi, M. Almutairi, K. Harb, O. Marey, Optimal Sizing Grid-Connected Hybrid PV/Generator/Battery Systems Following the Prediction of CO2 Emission and Electricity Consumption by Machine Learning Methods (MLP and SVR): Aseer, Tabuk, and Eastern Region, Saudi Arabia, Front. Energy Res. 10 (2022), 879373. https://doi.org/10.3389/fenrg.2022.879373.